CERES Angular Distribution Model Working Group Report

Wenying Su

Wenying.Su-1@nasa.gov

NASA LaRC, Hampton VA

Lusheng Liang Zachary Eitzen Sergio Sejas

SSAI, Hampton VA

From radiance to flux: angular distribution models

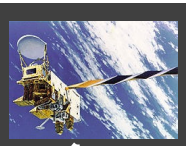

- Sort observed radiances into angular bins over different scene types;
- Integrate radiance over all θ and ϕ to estimate the anisotropic factor for each scene type:

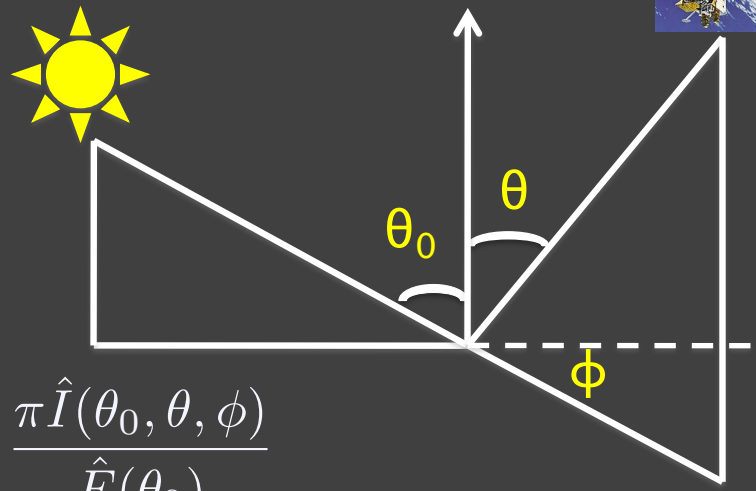

$$R(\theta_0,\theta,\phi) = \frac{\pi \hat{I}(\theta_0,\theta,\phi)}{\int_0^{2\pi}\int_0^{\frac{\pi}{2}} \hat{I}(\theta_0,\theta,\phi) cos\theta sin\theta d\theta d\phi} = \frac{\pi \hat{I}(\theta_0,\theta,\phi)}{\hat{F}(\theta_0)}$$

- For each radiance measurement, first determine the scene type, then apply scene type dependent anisotropic factor to observed radiance to derive TOA flux:

$$F(\theta_0) = \frac{\pi I_o(\theta_0,\theta,\phi)}{R(\theta_0,\theta,\phi)}$$

Snow and ice fraction used for scene identification

- Microwave-based snow/ice fraction from NSIDC/NESDIS
  - The NSIDC (National Snow and Ice Data Center) snow/ice map is from the Near-Real-Time SSM/I-SSMIS EASE-Grid Daily Global Ice Concentration and Snow Extent product (Near-real-time Ice and Snow Extent, NISE).
  - NESDIS snow/ice map is also produced using microwave data. It is only used when NSIDC data is not available.
- Imager-based snow/ice fraction from cloud mask algorithm
  - Snow/ice tests only apply to clear MODIS pixels
  - Snow/ice detection algorithms were developed separately for polar and non-polar regions using combinations of reflectance at 0.6 μm, 1.38 μm, 2.1 μm, and temperatures at 3.7 μm, 11 μm, 12 μm.

NSIDC and imager-based snow ice fraction differ

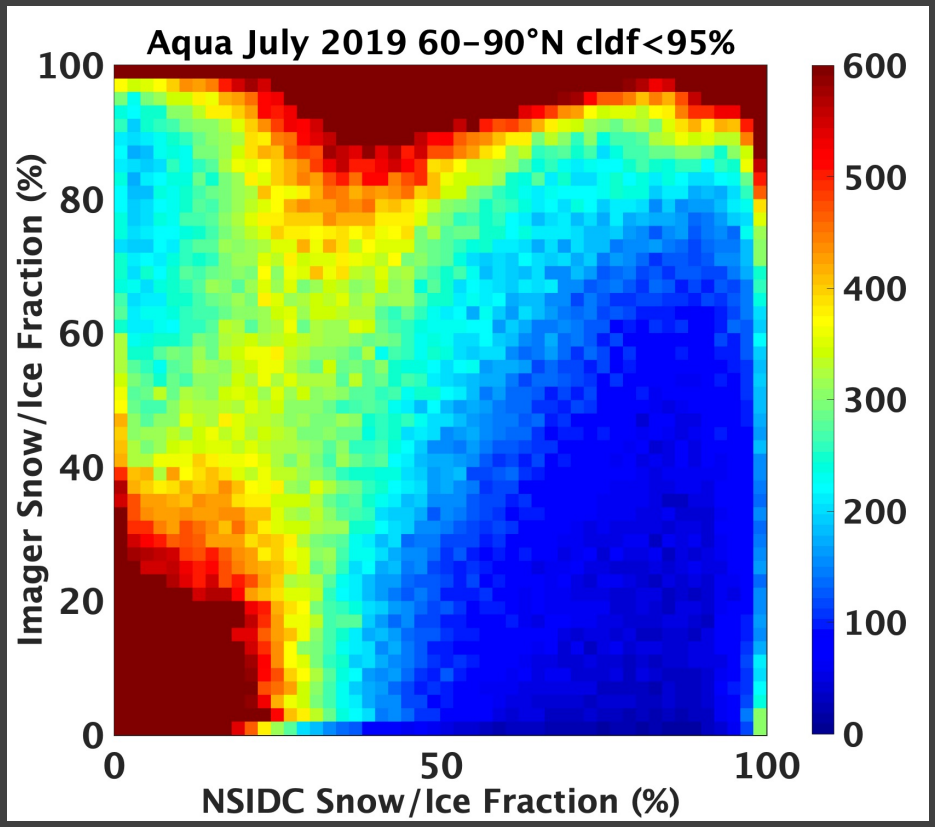

NSIDC mean=67.3%
Imager mean =84.5%
RMSE=30.6%

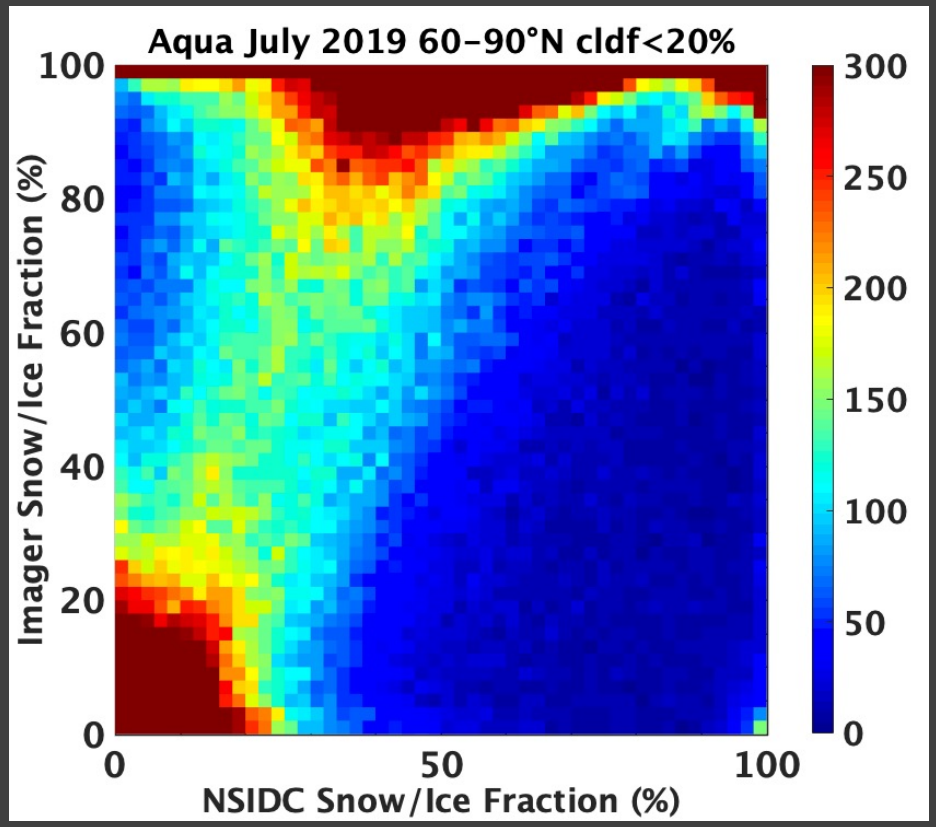

NSIDC mean=73.2%
Imager mean =87.3%
RMSE=25.4%

Sea ice fraction and CERES SW reflectance under clear-sky conditions

- Microwave product underestimates sea ice concentration
- Imager-based sea ice fraction overestimates sea ice concentration

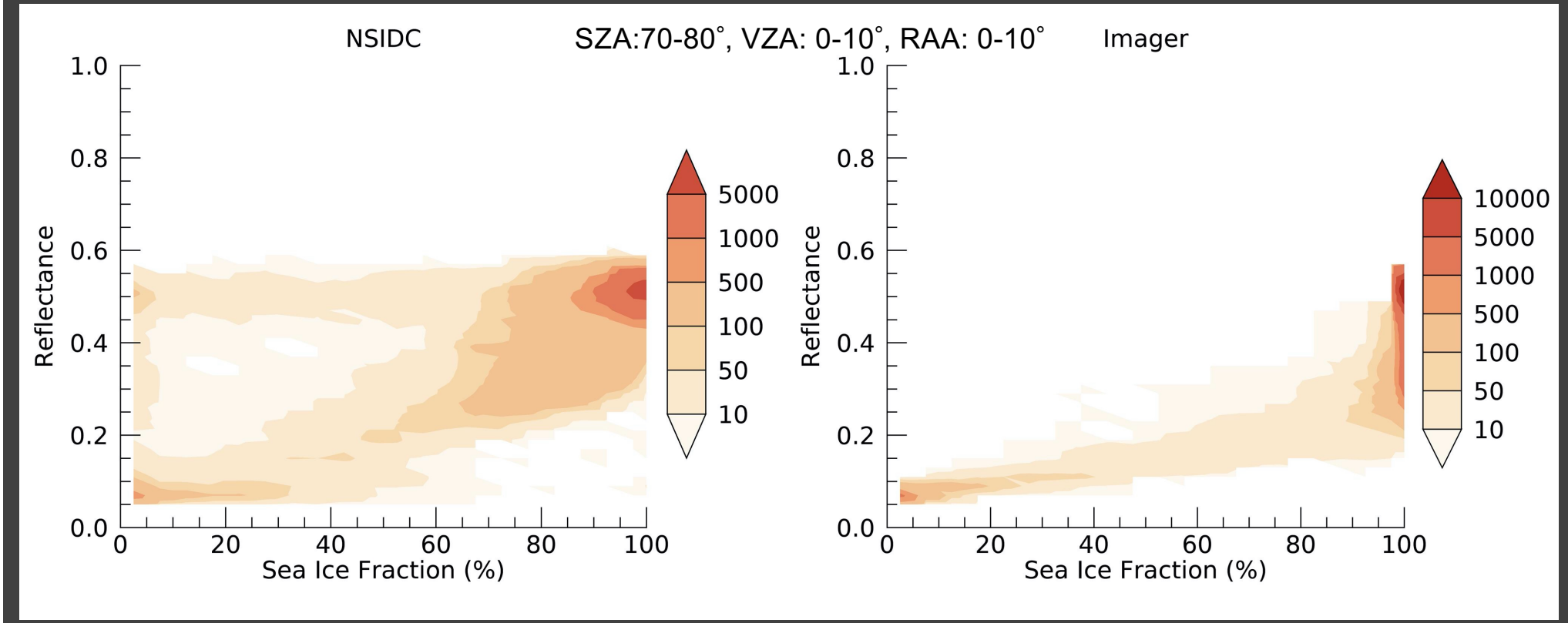

Validating sea ice concentration: Kern et al. (2019)

- Separate the 10 sea-ice concentration products into 4 groups based on retrieval concept.
- Used ship-based visual observations (7000 over Antarctic, and 8000 over Arctic) to validate each product.

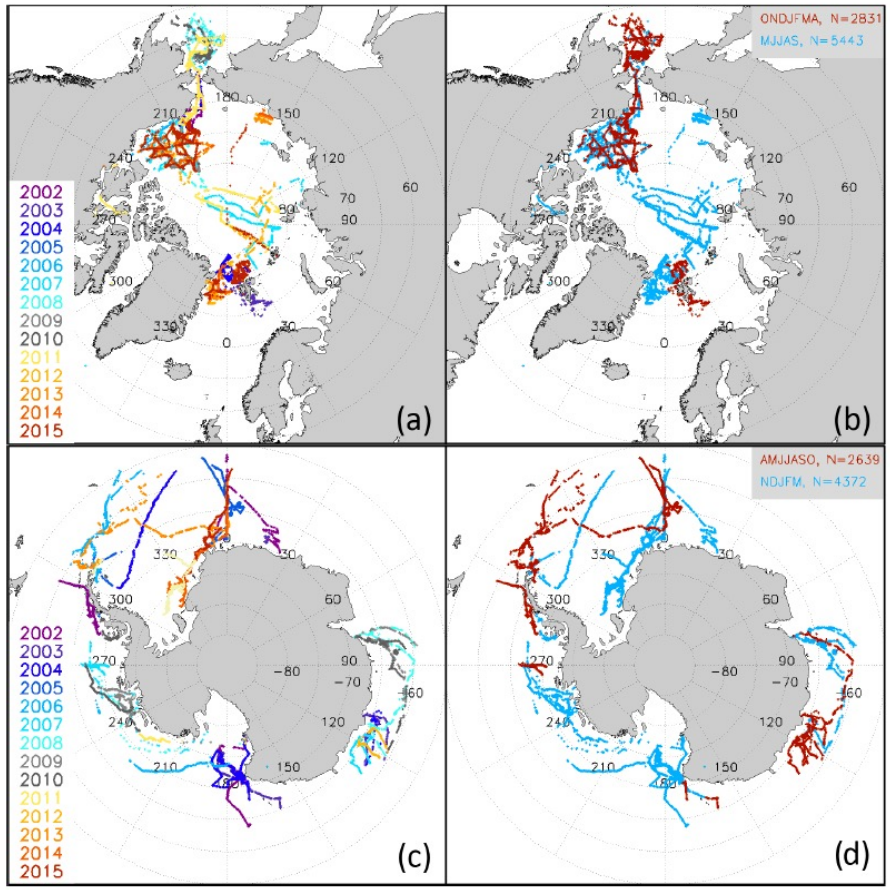

Figure 5. Spatio-temporal distribution of the ship tracks for **(a, b)** the Arctic and **(c, d)** the Antarctic from which ship-based visual observations of the sea-ice cover were used. Panels **(a, c)** illustrate the years, and panels **(b, d)** distinguish between winter (red) and summer (cyan) months.

Comparison between daily mean ship-based and satellite SIC for Arctic

Table 5. Summary of the statistics of the comparison between daily mean ship-based and satellite SIC data (see Fig. 15, black symbols) for – from top to bottom – the entire year, only winter and only summer. DIFF is the mean difference satellite minus ship-based SIC, and SD is the respective standard deviation; R^2 is the squared linear correlation coefficient. All concentration values are given in percent.

Group	I				II			III		IV
All year	SICCI-12km	SICCI-25km	SICCI-50km	OSI-450	CBT–SSMI	NOAA CDR	CBT–AMSR-E	ASI–SSMI	NT1–SSMI	NT2–AMSR-E
DIFF	−6.9	−7.8	−7.3	−7.3	+0.4	+0.6	−0.7	−5.4	−13.8	−0.7
SD	12.0	12.1	12.4	12.9	13.4	13.3	12.9	16.1	14.5	13.3
R^2	0.784	0.781	0.775	0.734	0.737	0.745	0.778	0.647	0.693	0.767
Winter										
DIFF	−7.4	−7.4	−6.2	−7.4	< |0.1|	−0.2	−1.5	−8.6	−14.2	−0.3
SD	12.6	11.8	11.8	12.8	10.9	11.6	12.6	17.4	13.8	11.5
R^2	0.558	0.594	0.606	0.591	0.595	0.587	0.551	0.429	0.507	0.595
Summer										
DIFF	−6.7	−8.0	−7.9	−7.3	+0.7	+0.9	−0.3	−3.7	−13.6	−0.9
SD	11.7	12.3	12.7	12.9	14.5	14.0	13.1	15.1	14.9	14.1
R^2	0.814	0.793	0.780	0.754	0.734	0.750	0.806	0.722	0.702	0.771

Currently in SSF

Comparison between daily mean ship-based and satellite SIC for Antarctic

Table 6. As Table 5 but for the Antarctic (see Fig. 16, black symbols).

Group	I				II			III		IV
All year	SICCI-12km	SICCI-25km	SICCI-50km	OSI-450	CBT–SSMI	NOAA CDR	CBT–AMSR-E	ASI–SSMI	NT1–SSMI	NT2–AMSR-E
DIFF	−3.0	−4.4	−3.1	−3.8	−1.8	−2.3	−1.4	−3.3	−11.0	+4.5
SD	13.4	13.8	14.0	13.7	15.2	15.5	14.8	15.7	14.8	16.9
R^2	0.763	0.745	0.737	0.733	0.711	0.716	0.755	0.671	0.698	0.679
Winter										
DIFF	−1.6	−2.7	−2.6	−3.2	−1.6	−2.0	+0.2	−3.6	−11.6	+3.8
SD	9.8	9.6	10.5	10.5	10.7	11.0	9.5	10.6	11.7	10.7
R^2	0.771	0.771	0.741	0.731	0.748	0.751	0.753	0.659	0.700	0.732
Summer										
DIFF	−3.9	−5.6	−3.4	−4.2	−2.0	−2.5	−2.5	−3.1	−10.6	+5.0
SD	15.3	16.1	16.0	15.6	17.7	17.9	17.4	18.4	16.6	20.0
R^2	0.698	0.666	0.675	0.667	0.643	0.651	0.693	0.614	0.640	0.621

Currently in SSF

Use sea ice brightness index to classify clear-sky ADMs

$$\eta = 1 - \frac{\rho_{0.47} - \rho_{0.86}}{\rho_{0.47} + \rho_{0.86}}$$

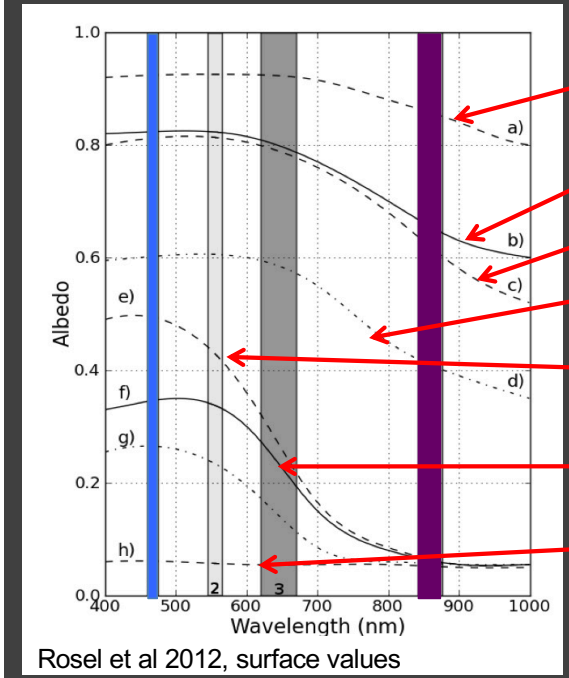

Rosel et al 2012, surface values

High sea ice index

Snow

Bare ice

Wet snow

Melting first year ice

~0.8-1.0

Young melting pond

Melting ponds

Open water

~0.1-0.5

Low sea ice index

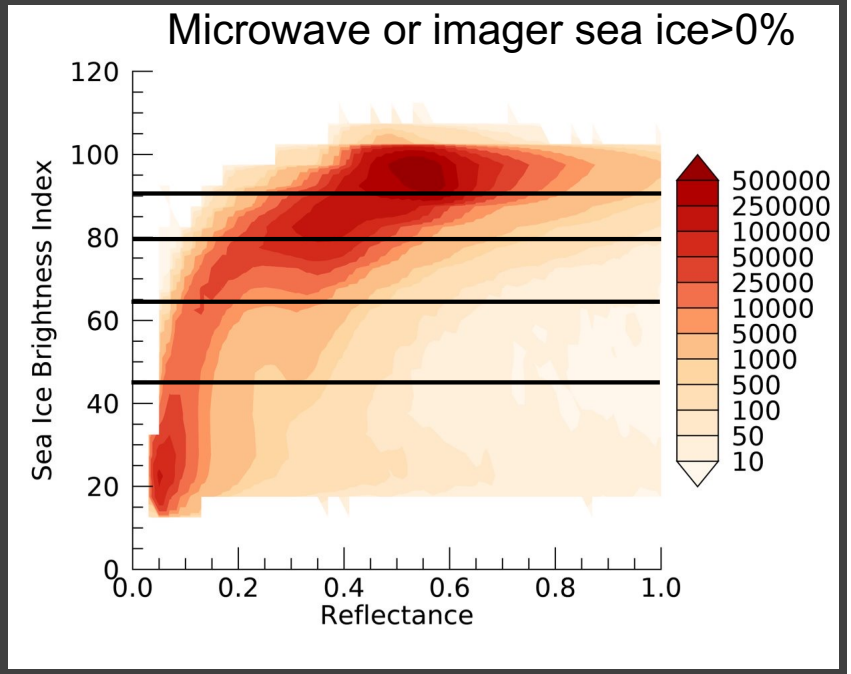

Using SIBI to classify the clear-sky sea ice ADMs increases flux consistency for clear sea ice scenes.

CERES unfiltering algorithm

- Filters are placed in front of the radiometers to measure the energies from the SW, WN/LW, and total portions of the spectrum. These filtered radiances are dependent upon how the radiation is filtered through the instrument optics.
- A procedure is applied that corrects for the spectral response of the instrument to produce "unfiltered" radiances that represent the radiation received by the instrument prior to entering the optics.
- Developed a more comprehensive database of spectral radiances to describe the relationship between filtered and unfiltered radiances.
- Includes more solar and viewing zenith angles.
- Seasonal simulations for different surface types (forest, savanna, grassland/crops, dark desert, and bright desert) using land surface BRDF from MODIS.
- Snow models are from Warren & Wiscombe, and MODIS Arctic and Antarctic BRDF model.
- Using median and percentile to specify AODs and surface temperatures when appropriate.

Impact of new unfiltering algorithm on instantaneous SW flux

Terra

Aqua

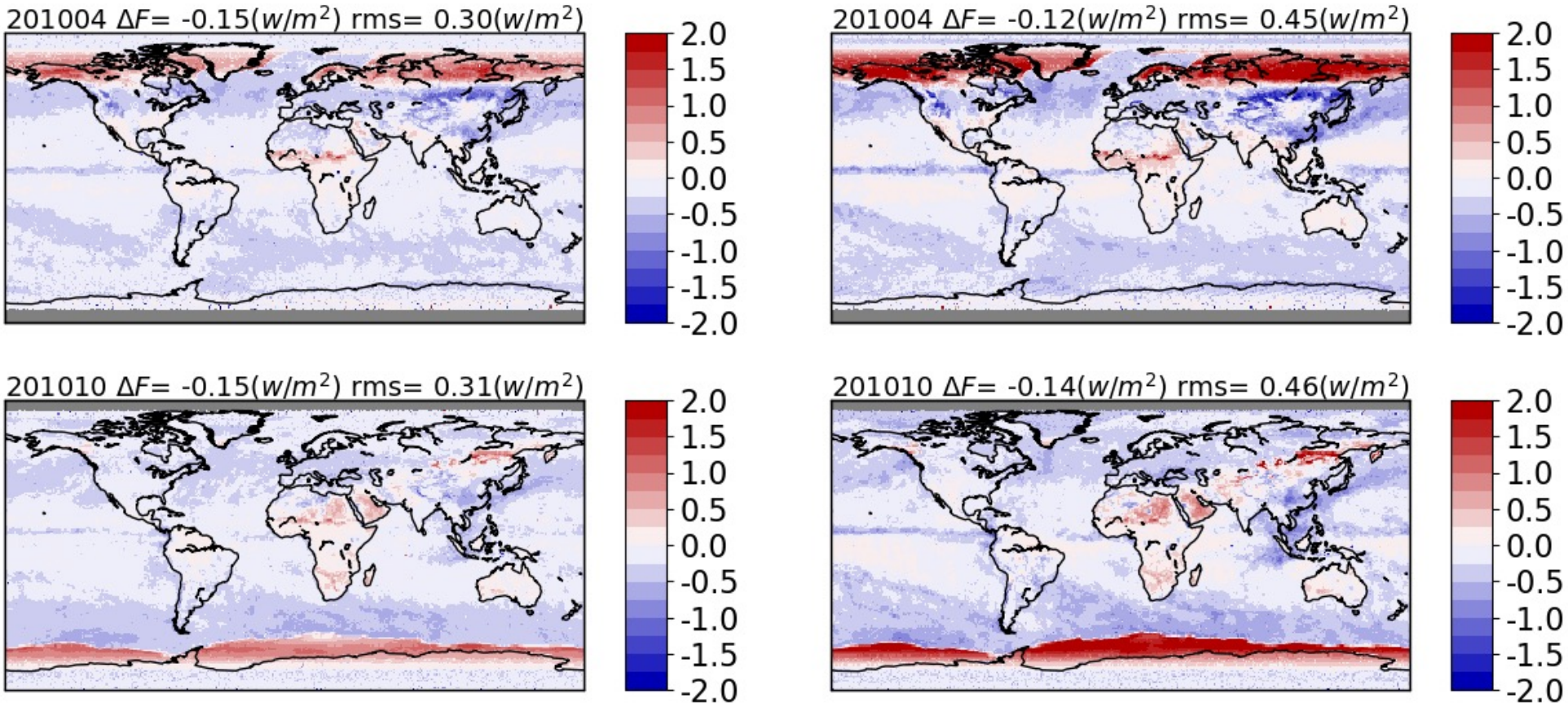

Δ=new-old

Impact of new unfiltering algorithm on daytime LW flux (TOT-SW)

Terra

Aqua

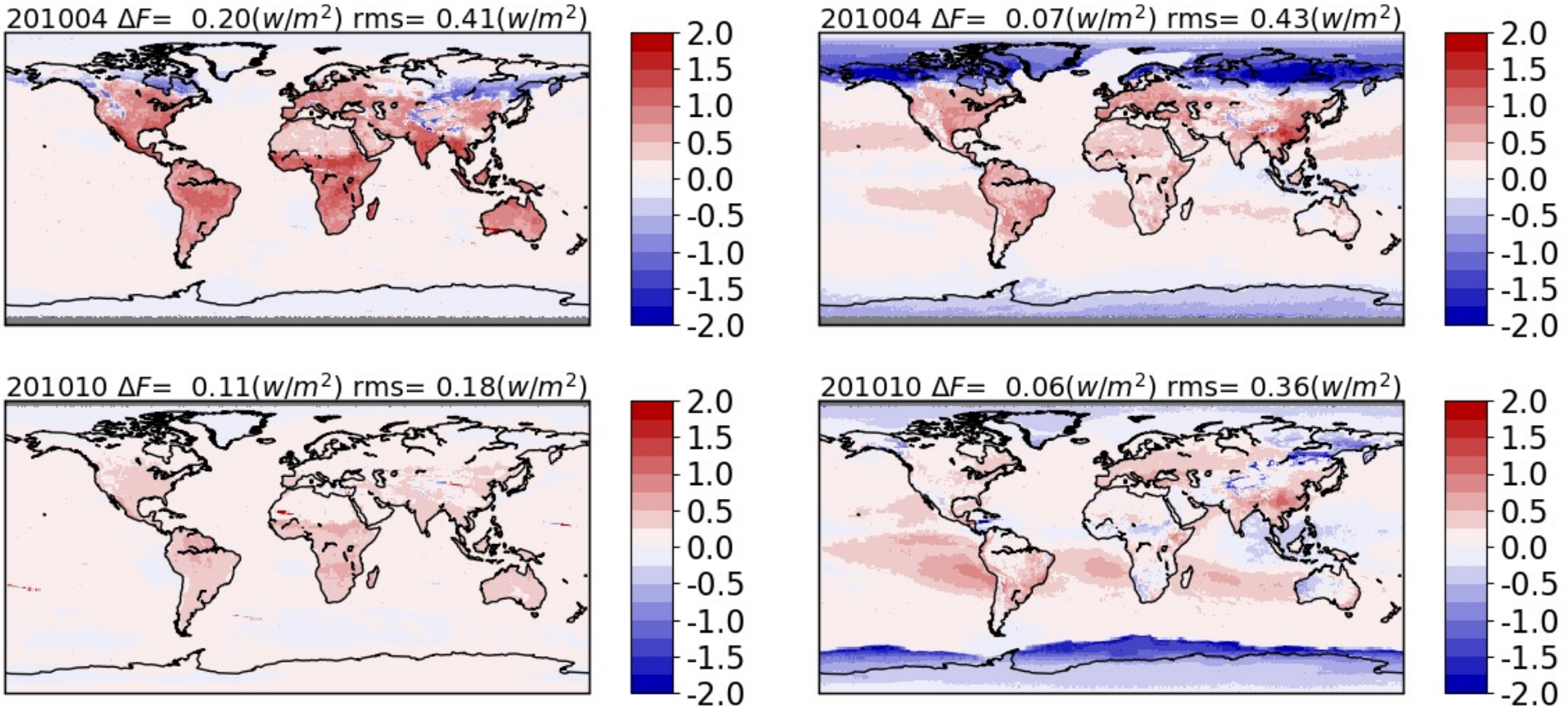

Impact of new unfiltering algorithm on nighttime LW flux (TOT)

Terra

Aqua

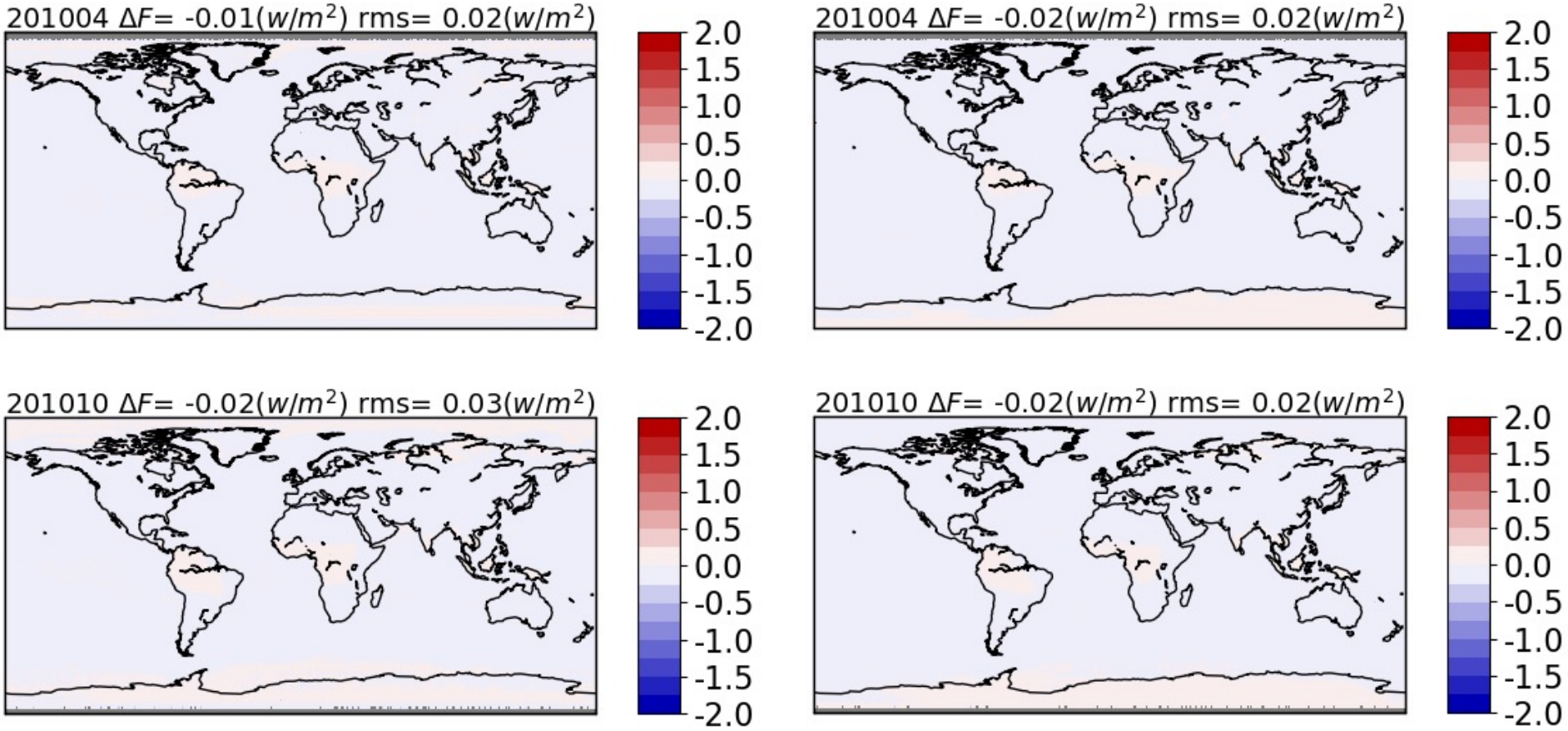

Error analysis database

- Extreme cases for ocean and land
  - Large aerosol loading (99th percentile)
  - Minimum/maximum surface temperatures
  - Wind speeds of 2 m/s and 12 m/s over ocean
  - Unfiltering clear-sky radiances assuming cloudy, and unfiltering cloudy scene assuming clear-sky
- Different aerosol types
- Different cloud types and optical depths for cloudy ocean and land
- Spectrally integrated unfiltered radiances are then compared with the "unfiltered" radiance derived from filtered radiances by using the regressions

SW radiance unfiltering uncertainty at different solar zenith angles

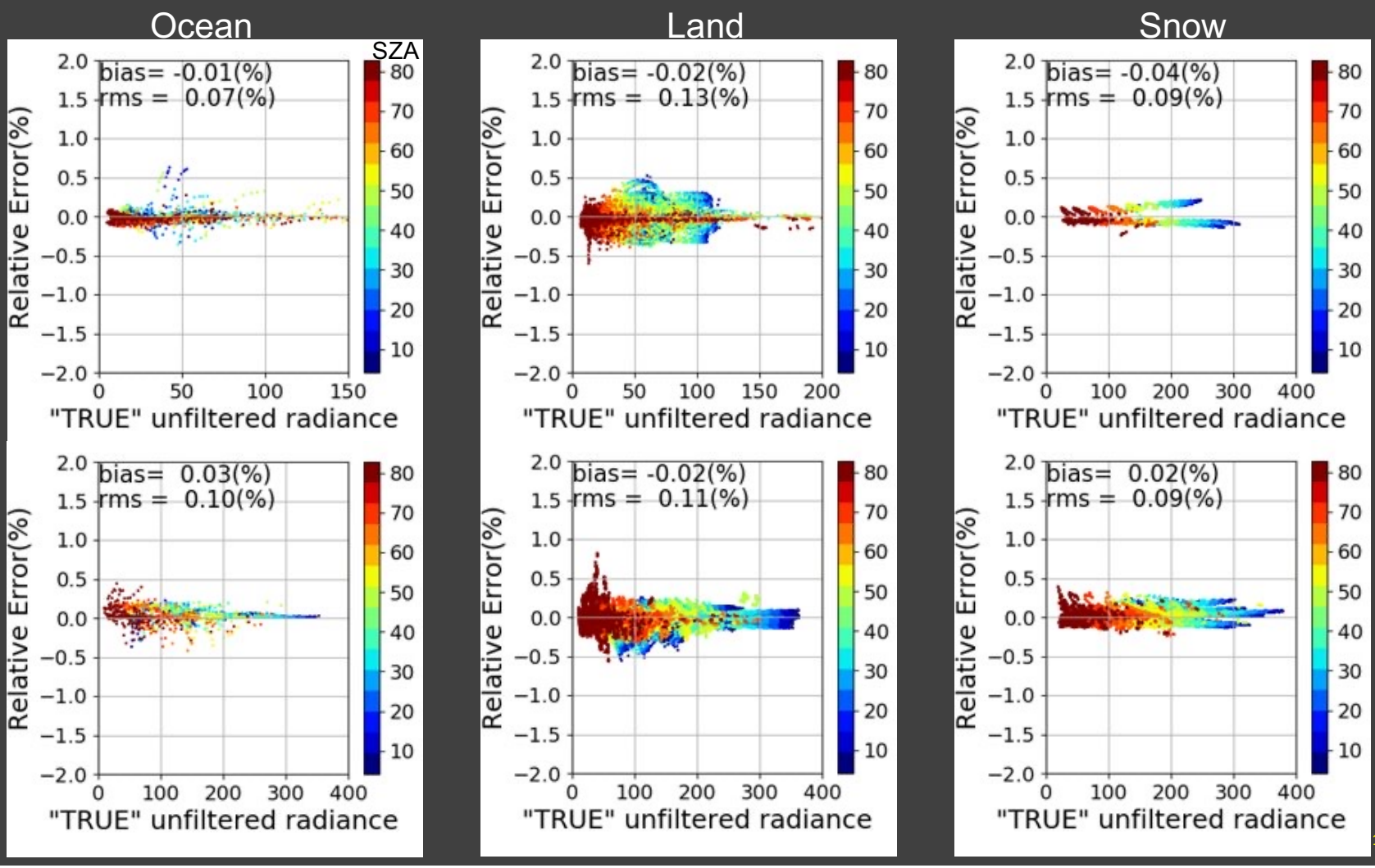

SW radiance unfiltering uncertainty to wind speed and aerosol type over clear ocean

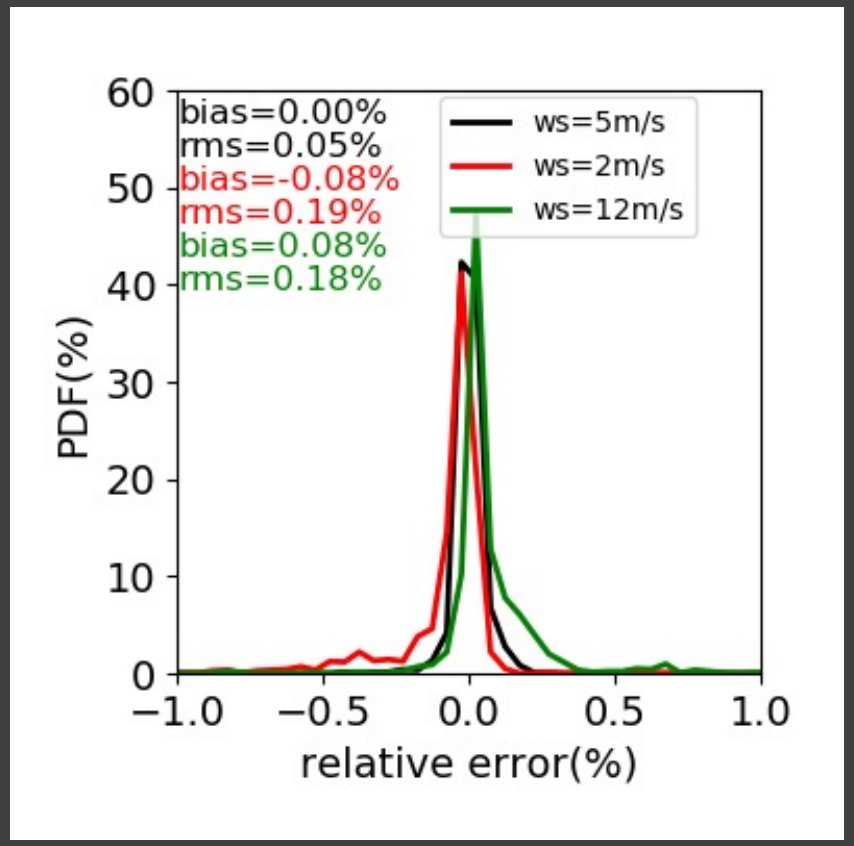

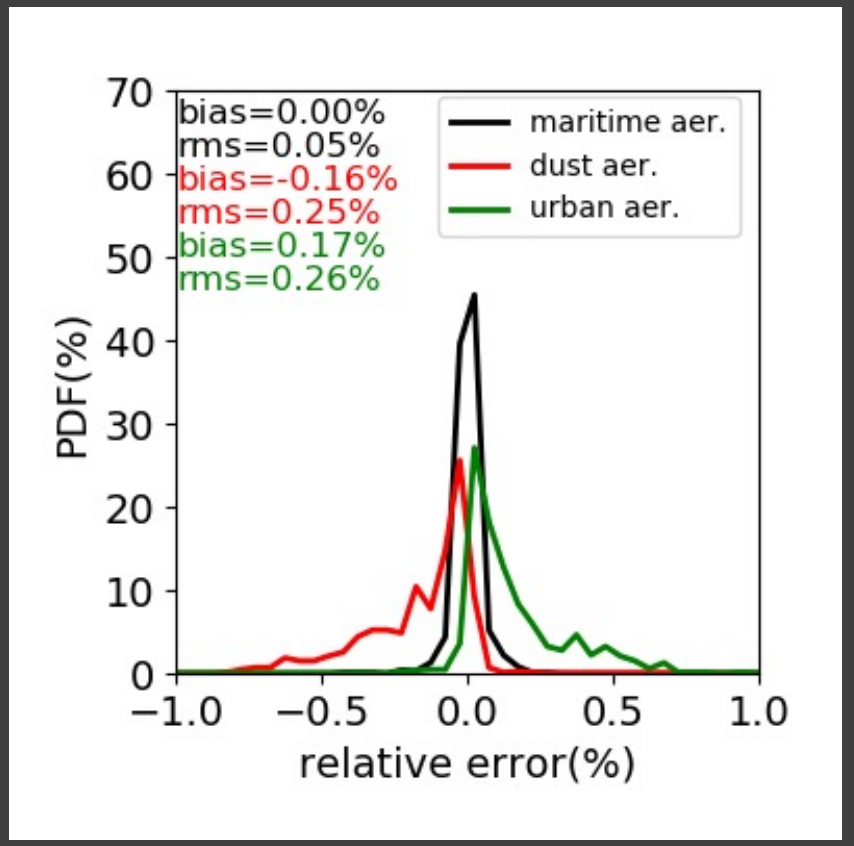

SW radiance unfiltering uncertainty to surface type and aerosol optical depth over clear land

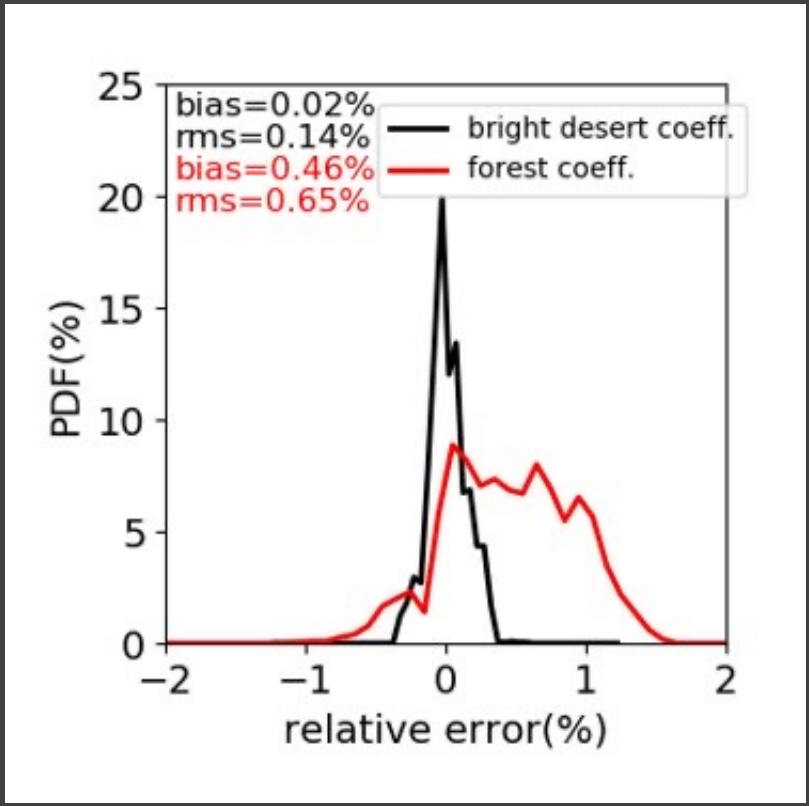

Applying unfiltering coefficients derived over forest to bright desert increases the uncertainty by a factor of 5

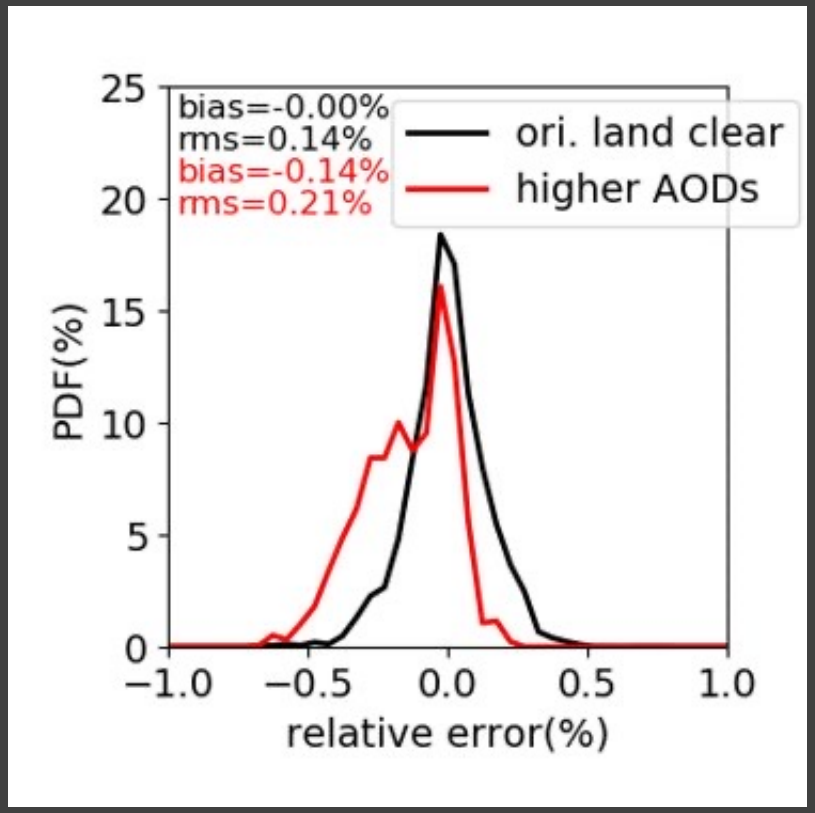

Unfiltering uncertainty distribution using median AOD and 99 percentile AOD

- **Median AODs range from 0.05 to 0.83**
- **99th percentile AODs range from 0.5 to 1.3**

SW radiance unfiltering uncertainty to cloud optical depth

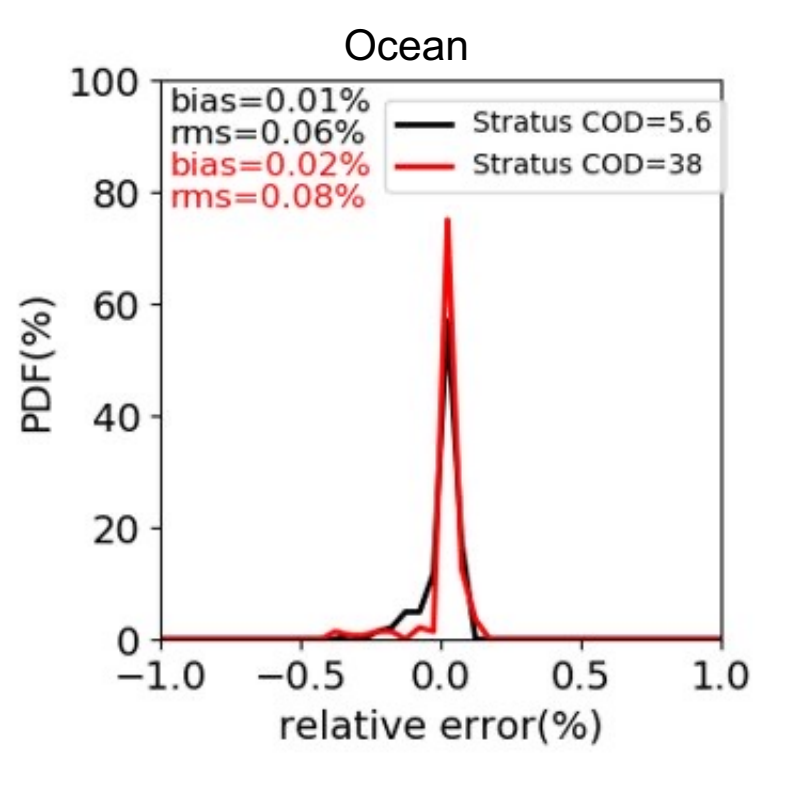

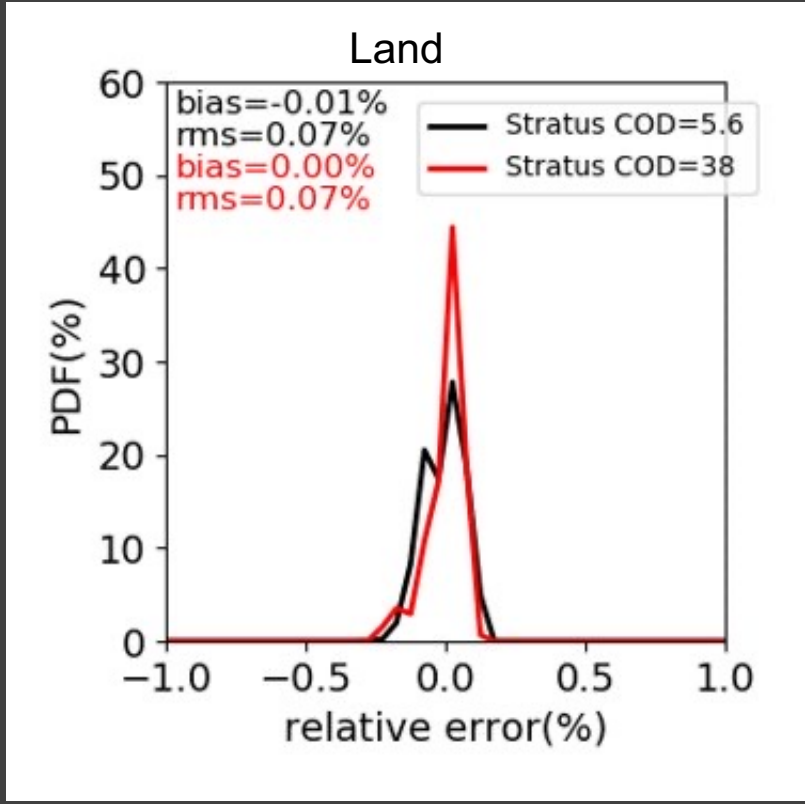

Daytime LW radiance unfiltering uncertainty to surface temperature

Ocean

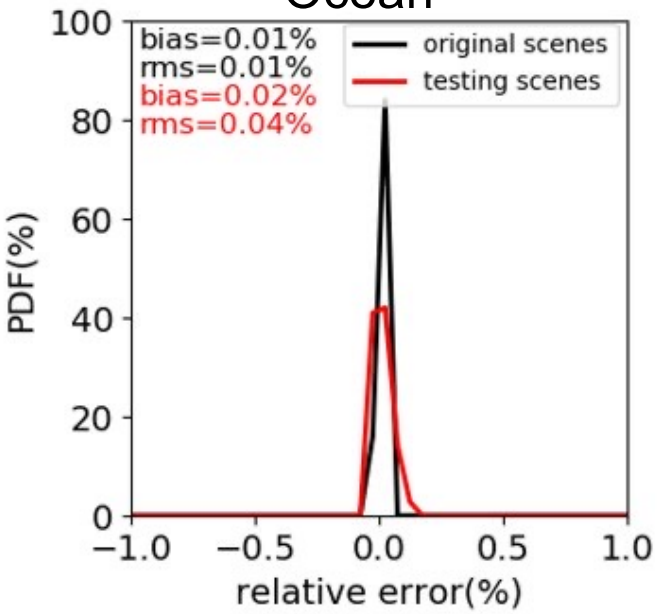

Land

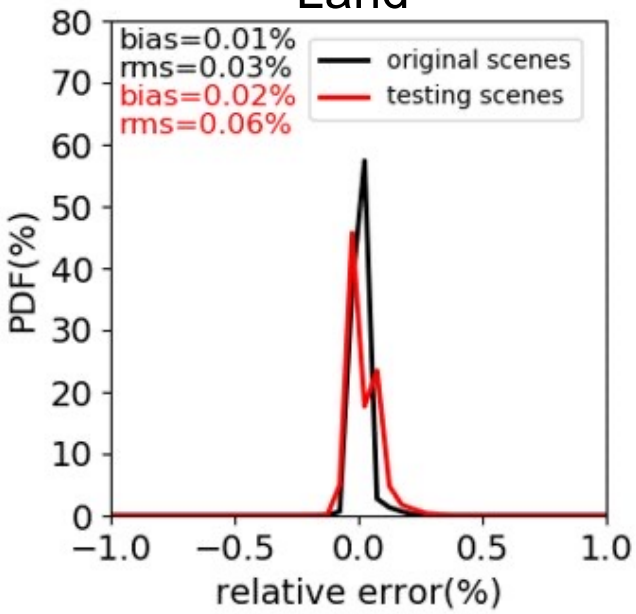

Snow

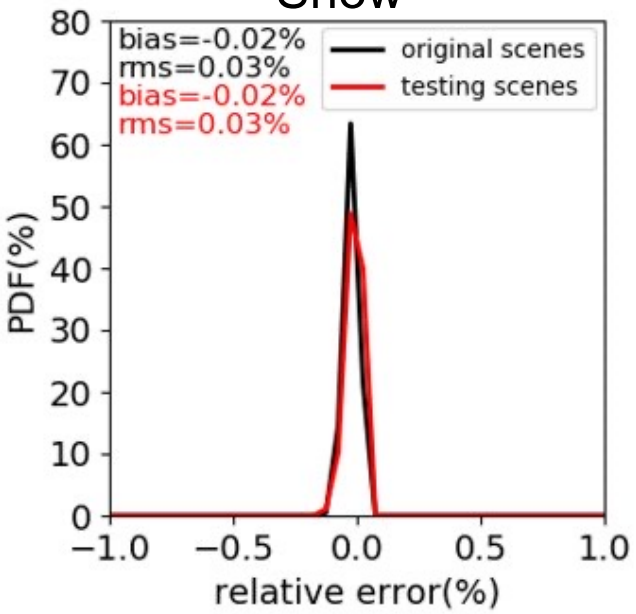

NPP ADMs: LW Clear-sky

- CERES on NPP has been collecting full RAP data since March 2020.
- CERES clear-sky LW ADMs are constructed separately over ocean, desert and non-desert land for discrete intervals of precipitable water, lapse rate, and surface skin temperature.

Table 3. Precipitable water (w), lapse rate (ΔT), and surface skin temperature (T_S) intervals used to determine LW and WN ADMs under clear-sky conditions over the ocean, land, and desert. There are 4 w bins, 4 ΔT bins, and 10 T_S bins.

w (cm)	ΔT (K)	T_S (K)
0–1	< 15	< 260
1–3	15–30	260–340 every 10 K
3–5	30–45	> 340
> 5	> 45	

Su et al. (2015)

Anisotropic factor comparisons between NPP and Aqua over clean scenes

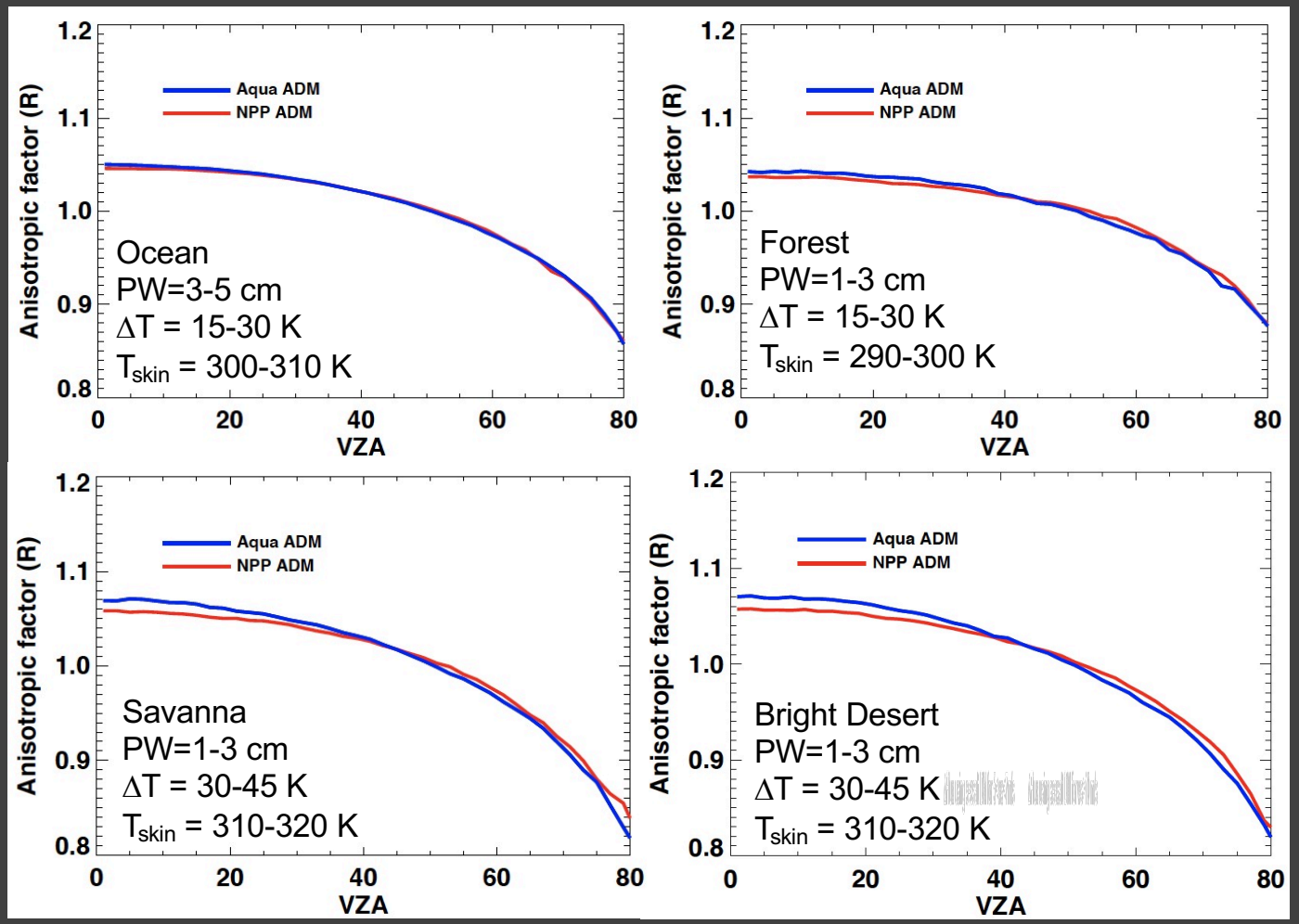

Cloudy-sky LW ADMs

- LW ADMs over cloudy-sky are constructed as a function of 'pseudoradiance' (Ψ) over discrete intervals of surface temperature, cloud fraction, precipitable water, etc.:

$$\Psi(w, T_s, T_c, f, \epsilon_s, \epsilon_c) =$$
$$(1-f)\epsilon_s B(T_s) + \sum_{j=1}^{2}\left[\epsilon_s B(T_s)(1-\epsilon_{c_j}) + \epsilon_{c_j} B(T_{c_j})\right] f_j$$

- For each given case, mean radiance for each 1 $Wm^{-2}sr^{-1}$ Ψ bin is calculated and a third-order polynomial fit is used as a backup.

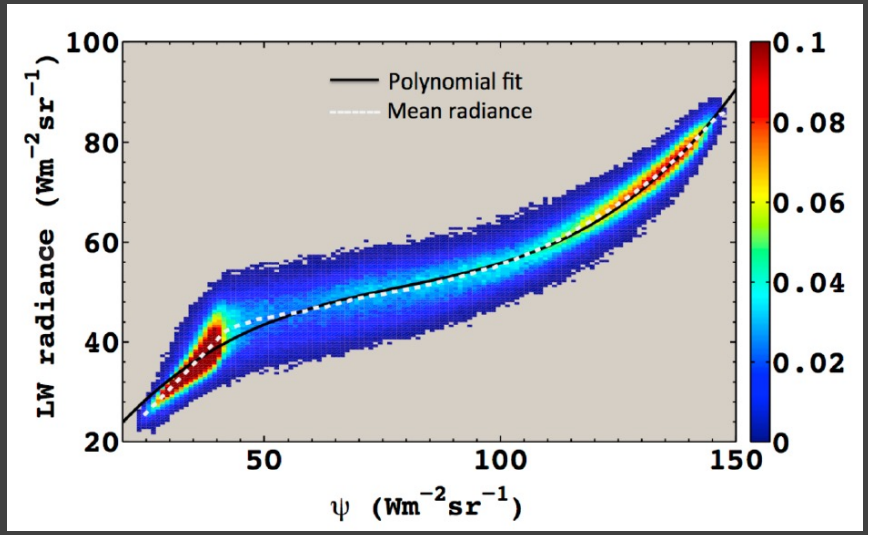

Table 5. Surface type, precipitable water (w), cloud fraction (f), surface–cloud temperature difference (ΔT_{sc}), and surface skin temperature (T_s) intervals used to determine LW and WN ADMs under cloudy conditions over the ocean, land, and desert surface. There are 4 w bins, 5 f bins, 22 ΔT_{sc} bins, and 11 T_s bins.

Surface type	w (cm)	f (%)	ΔT_{sc} (K)	T_s (K)
Ocean	0–1	0.1–25	< -15	< 275
Land	1–3	25–50	-15 to 85 every 5 K	275 to 320 every 5 K
Desert	3–5	50–75	> 85	> 320
	> 5	75–99.9		
		99.9–100		

Su et al. (2015)

Increasing pseudoradiance bin from 1 to 2 $Wm^{-2}sr^{-1}$ has minimum impact on monthly mean flux

- Construct LW ADMs using pseudoradiance bin of 2 W m^{-2} sr^{-1}
- Fluxes inverted with this sets of ADMs are virtually the same as Ed4 ADMs

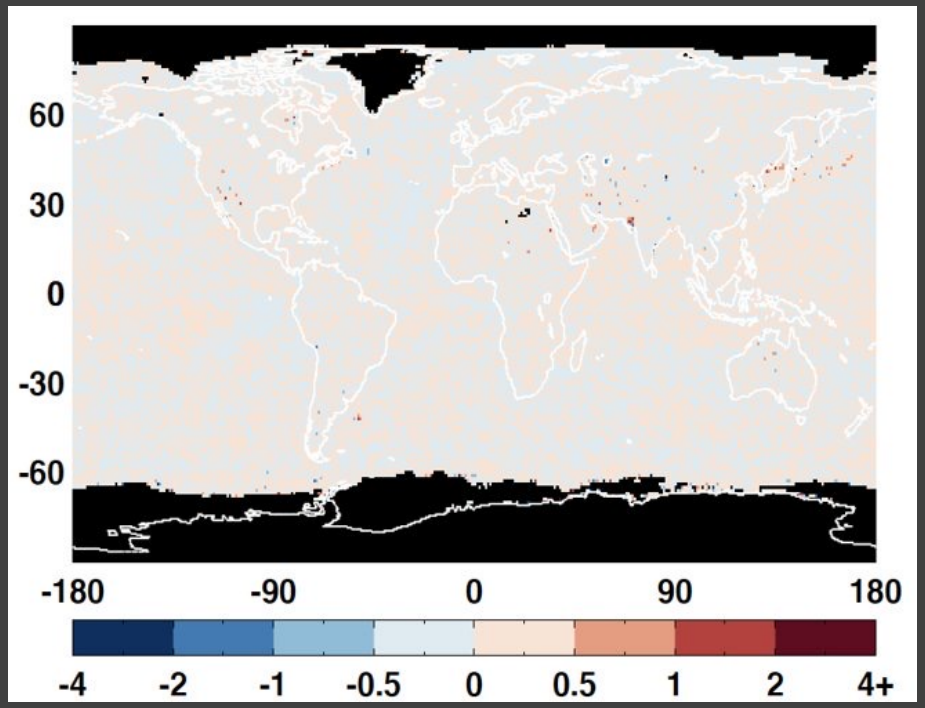

July 2018 flux differences

	Avg flux diff	RMS flux diff
Jan 2018	-0.002 W m^{-2}	0.11 W m^{-2}
Apr 2018	-0.002 W m^{-2}	0.10 W m^{-2}
Jul 2018	~0.000 W m^{-2}	0.09 W m^{-2}
Oct 2018	~0.000 W m^{-2}	0.08 W m^{-2}

Summary

- The current NSIDC sea ice concentration used in CERES data processing underestimates sea ice concentration by about 10%.
- Sea ice brightness index is used to mitigate this issue. NOAA sea ice concentration CDR is considered for Ed5.
- The updated unfiltering algorithm will be used for CERES Ed5. Error analysis indicates that the unfiltering uncertainty is less than 0.3% for SW and less than 0.1% for LW.
- The undated unfiltering algorithm has negligible impact on global mean fluxes, but regional instantaneous monthly mean SW and daytime LW flux can change by up to 2 Wm-2.
- Initial NPP clear-sky LW ADMs are more isotropic than Aqua ADMs.